Published in final edited form as:
Mol Cancer Ther. 2012 August ; 11(8): 1661–1671. doi:10.1158/1535-7163.MCT-12-0072.

Co-targeting stress-activated Hsp27 and autophagy as a combinatorial strategy to amplify endoplasmic reticular stress in prostate cancer

Masafumi Kumano[1,*], **Junya Furukawa**[2,*], **Masaki Shiota**[1], **Anousheh Zardan**[1], **Fan Zhang**[1], **Eliana Beraldi**[1], **Romina M. Wiedmann**[1], **Ladan Fazli**[1], **Amina Zoubeidi**[1], and **Martin E. Gleave**[1]

[1]The Vancouver Prostate Centre and Department of Urological Sciences, University of British Columbia, Vancouver, British Columbia, Canada

[2]Division of Urology, Kobe University Graduate School of Medicine, Kobe, Japan

Abstract

Heat shock protein-27 (Hsp27) is a stress-activated multifunctional chaperone that inhibits treatment-induced apoptosis and causes treatment resistance in prostate and other cancers. We previously showed that targeted suppression of Hsp27 sensitizes cancer cells to hormone and chemotherapy. However, mechanisms by which Hsp27 confers cell treatment resistance are incompletely defined. Here, we report that Hsp27 protects human prostate cancer cells against proteotoxic stress induced by proteasome inhibition, and that Hsp27 silencing using siRNA or antisense (OGX-427) induced both apoptosis and autophagy through mechanisms involving reduced proteasome activity and induction of endoplasmic reticulum (ER) stress. We found that autophagy activation protected against ER stress-induced cell death, while inhibition of autophagy activation following Hsp27 silencing using either pharmacological inhibitors or atg3 silencing enhanced cell death. Importantly, co-targeting Hsp27 and autophagy by combining OGX-427 with the autophagy inhibitor, chloroquine, significantly delayed PC-3 prostate tumor growth in vivo. These findings identify autophagy as a cytoprotective, stress-induced adaptive pathway, activated following disruption of protein homeostasis and ER stress induced by Hsp27 silencing. Combinatorial co-targeting cytoprotective Hsp27 and autophagy illustrates potential benefits of blocking activation of adaptive pathways to improve treatment outcomes in cancer.

Keywords

prostate cancer; Hsp27; proteasome; UPR; autophagy

Corresponding Author: Martin E. Gleave, Department of Urologic Sciences, University of British Columbia, 2775 Laurel Street, Level 6, Vancouver, British Columbia, Canada V6H 3Z6. m.gleave@ubc.ca.
*These authors contributed equally to this work

Disclosure of Potential Conflicts of Interest

By way of disclosure of conflict of interest, The University of British Columbia has submitted patent applications on OGX-427, listing Drs Gleave as inventor. This IP has been licensed to OncoGenex Technologies, a Vancouver-based biotechnology company that Dr. Gleave has founding shares in.

INTRODUCTION

Many strategies used to kill cancer cells induce stress-responses that promote the emergence of a treatment resistant phenotype. In prostate cancer (PCa), androgen ablation induces remission in most patients but also progression to castration resistant prostate cancer (CRPC) [1]. While docetaxel chemotherapy [2] and more recently AR pathway inhibitors like abiraterone [3] and MDV-3100 prolong survival by several months, treatment resistance frequently emerges, highlighting the need for additional therapies targeting the molecular basis of CRPC and treatment resistance.

Development of CRPC is attributed to re-activation of the androgen receptor (AR) axis [4], alternative growth factor pathways [5], stress-induced survival genes [6], and cytoprotective chaperone networks [7]. Molecular chaperones like heat-shock proteins (Hsps) help cells cope with stress-induced misfolded proteins and play prominent roles in cellular signaling and transcriptional regulatory networks. In particular, Hsp27 is a stress-activated chaperone highly expressed in CRPC and other cancers that inhibits treatment-induced apoptosis [8–10]. Hsp27 is induced by anti-AR and chemotherapy, inhibiting apoptosis by regulating components of both stress- and receptor-induced apoptotic pathways [11–14]. We previously reported that Hsp27 silencing induces apoptosis and enhances anticancer drug sensitivity in prostate and bladder cancer cells [7, 15–16]. The Hsp27 inhibitor, OGX-427, delays progression and enhances activity of chemotherapy in CRPC and other cancers [7, 15–16], and is currently in multicenter Phase II studies of CRPC and metastatic bladder cancer (ClinicalTrials.gov identifier, NCT01454089 and NCT01120470).

Hsps are particularly important in regulating misfolded protein and endoplasmic reticular (ER) stress responses, an emerging area of interest in cancer progression and treatment resistance [17]. In cancer, ER stress and misfolded protein levels are elevated because of mutated genes and stressed microenvironments [18]; moreover, many anti-cancer agents induce ER stress [19]. ER stress activates a complex intracellular signaling pathway, called the unfolded protein response (UPR), tailored to reestablish protein homeostasis (proteostasis) by inhibiting protein translation and promoting ER-associated protein degradation (ERAD) by stimulating the ubiquitin-proteasome system (UPS) and autophagy to reduce levels of misfolded proteins [20]. Autophagy is an evolutionarily conserved bulk degradation system that facilitates clearance of stress-induced misfolded or aggregated proteins, as well as organelles [21]. Classically, autophagy is activated in starvation or oxidative stress and generally considered an adaptive survival mechanism [22]; however, when ER stress and unfolded protein burden overwhelms the degradation capacity of the proteasome or autophagy, then cell death can occur.

While many studies link UPS inhibition and ER stress to autophagy induction [23–26], whether treatment-induced autophagy is cytoprotective to facilitate development of acquired treatment resistance, or alternatively mediates treatment-induced cell death, remain controversial. Since Hsp27 has been identified as a cytoprotective chaperone linked to treatment resistance and cell survival [7, 11, 27–28], as well as ER stress and UPS activity [12, 29], we set out to explore its role in treatment-induced ER stress and protein homeostasis in PCa.

MATERIALS AND METHODS

Prostate Cancer Cell Lines and Reagents

LNCaP and C4-2 cells were kindly provided by Dr. Leland W. K. Chung (Cedar Sinai, Los Angeles) tested and authenticated by whole-genome and whole-transcriptome sequencing on Illumina Genome Analyzer IIx platform in July 2009. PC-3 cells were purchased from the American Type Culture Collection (2008, ATCC-authentication by isoenzymes analysis). LNCaP and C4-2 cells were maintained in RPMI-1640 media (Invitrogen Life Technologies) containing 5% heat inactivated fetal bovine serum (FBS; Invitrogen Life Technologies). PC-3 cells were maintained in Dulbecco's modified Eagle's medium (DMEM; Invitrogen Life Technologies) containing 5% FBS. PC-3 cells stably transfected with Hsp27 (PC-3_{Hsp27}) and empty vector-transfected PC-3 cells (PC-3_{Empty}) were generated as previously reported [13]. MG132 was purchased from Calbiochem (Darmstadt, Germany). Chloroquine (CQ), Bafilomycin and 3-Methyladenine (3-MA) were purchased from Sigma-Aldrich. Antibodies: anti-GRP78, anti-CREB2 (ATF4), anti-GADD153 (CHOP) and anti-Ubiquitin from Santa Cruz Biotechnology; anti-phospho-eIF2α from Invitrogen Life Technologies; anti-ATF6 from Imgenex Corp; anti-HSP27 from StressGen; anti-cleaved PARP, anti-phospho-HSP27 (Ser82), anti-Atg3 and anti-LC3 from Cell Signaling Technology; and anti-Vinculin and anti-β-Actin from Sigma-Aldrich.

ASO and siRNA Transfection

Cells were transfected with antisense or siRNA as described previously [27–28]. Hsp27 antisense oligonucleotide (ASO), OGX-427 was kindly provided by OncoGenex Pharmaceuticals, (Vancouver, BC). The sequence of OGX-427 corresponds to the human Hsp27 translation initiation site (5′-GGGACGCGGCGCTCGGTCAT-3′). A scrambled (ScrB) control oligonucleotide was generously provided by ISIS Pharmaceuticals (Carlsbad, CA). The sequence of Hsp27 small interfering (si) RNA corresponds to the human Hsp27 site (5′-GUCUCAUCGGAUUUUGCAGC-3′; Dharmacon). The sequence of Atg3 siRNA corresponds to the human Atg3 site (5′-GGAAUCAAAGUUUAAGGAAACAGGU-3′; Invitrogen Life Technologies). A scrambled siRNA (5′-CAGCGCUGACAACAGUUUCAU-3′; Dharmacon) was used as a control for RNA interference experiments.

Western Blotting Analysis

Total proteins were extracted using RIPA buffer (50mM Tris, pH 7.2, 1% NP-40, 0.1% deoxycholate, 0.1% SDS, 100mM NaCl, Roche complete protease inhibitor cocktail) and submitted to western blot as we described previously [27].

Proteasome Activity

Peptidase activity of the proteasome was measured by mixing tissue homogenate with 20 μM fluorogenic peptide Suc-LLVT-AMC (succinyl-Leu-Leu-Val-Tyr-7-amino-4-methylcoumarin) (Calbiochem) as we previously described [30].

Analysis of Xbp-1 splicing

Total RNA was isolated using Trizol reagent according to the manufacturer instructions (Life, Technology). cDNA was synthesized from 2 ug of RNA using the Superscript II First –strand synthesis kit (Invitrogen) and amplified with a pair of primers corresponding to nucleotides 285 -308 (forward) (5′-AAACAGAGTAGCAGCTCAGACTGC-3′) and-735–758 (reverse) (5′-TCCTTCTGGGTAGACCTCTGGGAG-3 ′) of X B P-1 cDNA. β actin (forward: GGACTTCGAGCAAGAGATGG; reverse: AGCACTGTGTTGGCGGTACAG) was used as endogenous control. PCR products were analyzed on 2.5% agarose gel.

In Vitro Cell Growth Assay

Cells were plated in 12-well plate, allowed to attach for 24 hrs, and treated with indicated concentrations of siRNA for 1 day or ASO for 2 days. Cell growth was then assessed using crystal violet assay as described previously [31]. Absorbance was determined with a microculture plate reader (Becton Dickinson Labware) at 560 nm, and the percentage of cell growth was calculated relative to vehicle-treated cells. Each assay was performed in triplicate.

Cell Cycle Analysis

Cell cycle populations were analyzed by propidium iodide–staining using a FACSCAN flow cytometer (Becton-Dickinson & Co., San Jose, CA) as previously described [28].

Immunofluorescence Staining

Cells were fixed with methanol containing 3% acetone and immunofluorescence was performed as previously described [27–28, 30] using anti-LC3 antibody (1:250, Cell Signaling Technology). Puncta from 100 to 150 cells were counted from 3 independent experiments for quantitative analysis as described previously [32]. Cells displaying >15 brightly fluorescent LC3 puncta were counted as positive. Photo-micrographs were taken at 40x magnification using Zeiss Axioplan II fluorescence microscope.

Immunohistochemistry

Immunohistochemistry was performed on formalin-fixed, paraffin-embedded 4-μm sections of tumor samples. Immunohistochemical staining was conducted using Hsp27 for target expression, Ki-67 for cell proliferation, TUNEL for apoptosis antibody in the Ventana autostainer Discover XT (Ventana Medical System) with enzyme-labeled biotin streptavidin system and solvent resistant 3,3′-diaminobenyidine Map kit. All comparisons of staining intensities were made at 200× magnifications.

Assessment of In Vivo Tumor Growth

For in vivo xenograft studies, PC-3 cells were inoculated s.c. in the flank of 6- to 8-week-old male athymic nude mice (Harlan Sprague Dawley, Inc.) via a 27-gauge needle under isoflurane anesthesia. When PC-3 tumors reached 100mm^3, mice were randomly selected to one of 4 groups for treatment with 50mg/kg chloroquine i.p. once daily 5 days per week alone or in combination with 15 mg/kg OGX-427 or ScrB injected i.p. once daily for 7 days and then 3 times per week thereafter. Each experimental group consisted of 8 mice. Tumor

volume measurements were performed once weekly and calculated by the formula length × width × depth × 0.5236. Data points were expressed as average tumor volume ± SEM. All animal procedures were performed according to the guidelines of the Canadian Council on Animal Care and with appropriate institutional certification.

Statistical Analysis

Differences between the two groups were compared using Student's t-test and Mann-Whitney U test. All statistical calculations were performed using Statview 5.0 software (Abacus Concepts, Inc.), and P values < 0.05 were considered significant.

RESULTS

Hsp27 attenuates MG132 induced ER stress and apoptosis

While Hsp27 has been reported to confer resistance to proteasome inhibition in lymphoma cells [33] the underlying mechanisms remain undefined. Here, we show that the proteasome inhibitor MG132 induces up-regulation of Hsp27 and pHsp27 in the PC-3 cells (Fig. 1A). PC-3 cells stably overexpressing Hsp27 show similar cell growth and apoptotic rates compared to parental or empty vector under basal, unstressed conditions (Supplementary Fig. S1), moreover PC-3 and LNCaP cells overexpressing Hsp27 acquire resistance to MG132-induced apoptosis as shown by decreased sub G0 population (Fig. 1B, Supplementary Fig. S2A), increased cleaved-PARP and -caspase3 expression (Fig. 1C) and decreased cell growth rates (Fig. 1D and Supplementary Fig. S2B). Since MG132 is known to induce ER stress by inhibiting the ubiquitin-proteasomal system (UPS) [34], we next investigated role of Hsp27 on MG132-induced ER stress response and activation of the UPR. PC-3_{Hsp27} and PC-3_{Empty} were treated with indicated concentrations MG132 and expression of UPR related proteins analyzed. Hsp27 overexpression ameliorated MG132-induced ER stress and UPR activation of GRP78, ATF4, CHOP and cleaved-ATF6 compared to empty vector (Fig. 1C). Interestingly this effect correlated with increased proteasome activity and reduced accumulation of ubiquitinated proteins in PC-3_{Hsp27} compared to PC-3_{Empty} or PC-$3_{parental}$ cells, consistent with prior reports [12, 29] (Fig. 1E). We also observed that the Hsp90 inhibitor, 17-AAG, also induced ER stress and up-regulation of Hsp27 in LNCaP cells (Supplementary Fig. S2C) and that Hsp27 overexpression also conferred resistance to Hsp90 inhibitor-induced apoptosis (Supplementary Fig. S2D). These data suggest that Hsp27 functions to help maintain protein homeostasis under ER stress condition by increasing UPS activity and enhancing clearance of ubiquitinated proteins.

Hsp27 inhibition reduces UPS Activity and induces ER stress

To further define the role of Hsp27 in ER stress and UPR activation, levels of UPR-related proteins were analyzed by western blot after Hsp27 knockdown using siRNA or the antisense drug, OGX-427. We found that Hsp27 knockdown in PC-3 cells using siRNA (Fig. 2A, left panel) or OGX-427 (Fig. 2A, right panel) leads to up-regulation of GRP78, phospho-eIF2α, ATF4, CHOP and cleaved-ATF6 protein levels; similar effects were seen in LNCaP cells (Supplementary Fig. S3). In addition, spliced-XBP1 was detected (Fig. 2B). Spliced-XBP1 is a transcription factor that binds to UPR-responsive promoter elements in a

subset of genes to stimulate expression of chaperones as a mechanism to cope with the unfolded protein load [35]. Moreover, we observed that siRNA-Hsp27 (Fig. 2C, left panel) or OGX-427 (Fig. 2C, right panel) decreased proteasome activity and led to accumulation of ubiquitinated proteins. These results indicate that Hsp27 knockdown decreases proteasome activity, induces ER stress, and activates the UPR.

Hsp27 knockdown induces autophagy in PC-3 cells

Recent reports have defined mechanistic links between the UPS and autophagy-lysosome systems in proteostasis [36–37]. Since inhibition of the proteasome can activate autophagy [23], we explored whether Hsp27 inhibition induces autophagy using a variety of assays. LC3-II expression, which is a microtubule-associated protein light chain 3 and a marker of autophagy, was induced in a time-dependent manner after Hsp27 knockdown using siRNA (Fig. 3A, left panel), or OGX-427 (Fig. 3A, right panel). Interestingly, we observed that induction of autophagy correlates strongly with the extent of Hsp27 knockdown, which is achieved more potently with siRNA compared to OGX-427. Next, autophagic flux was analyzed using LC3 turnover assay [38]. Since Bafilomycin (Fig. 3B upper panel) blocks the fusion of autophagosome and lysosome, LC3-ll degradation in autolysosomes is also blocked and results in LC3-ll accumulation. Hsp27 knockdown using siRNA (Fig. 3B, lower left panel) or OGX-427 (Fig. 3B, lower right panel) increased autophagic flux with higher LC3-II levels after bafilomycin treatment. To further evaluate changes in autophagic flux after Hsp27 knockdown, we quantified green fluorescence puncta of endogenous LC3 in PC-3 cells. As expected, Hsp27 knockdown significantly increased LC3 puncta compared to controls (Fig. 3C). Collectively, these data indicate that Hsp27 knockdown inhibits proteasome activity and results in increased autophagic flux in PC-3 cells.

Co-targeting Hsp27 and autophagy enhances PCa cell death

Recent studies indicate that autophagy activation in cancer cells is context-dependent and can be either cytoprotective or a mediator of apoptosis [23–24, 39–40]. Since Hsp27 knockdown induces ER stress and autophagy, we next examined effects of inhibition of autophagy on apoptotic rates after OGX-427 treatment in PCa cells. First, we confirmed that OGX-427 induces autophagy in other PCa cell lines by measuring autophagic flux in LNCaP and C4-2 PCa cell lines (Fig. 4A). Next, we evaluated the effect of autophagy inhibition using 3-methyladenine (3-MA) or chloroquine (CQ) after OGX-427-induced ER stress in these PCa cell lines. 3-MA inhibits the activity of class III PI3 kinases required for autophagosome formation, while CQ is an anti-malaria drug that inhibits autophagosome–lysosome fusion and lysosomal acidification, resulting in inhibition of autophagy and LC3-ll degradation. As shown in Figure 4B, either CQ or 3-MA significantly enhanced the cell-growth inhibitory effects of OGX-427 in PCa cell lines. Also, combined OGX-427 plus CQ, compared to CQ or OGX-427 monotherapy, significantly increased apoptotic rates as measured by cleaved PARP (Fig. 4C, left panel and Supplementary Fig. S4) and flow cytometric analysis (Fig. 4C, right panel) in PC-3 cells. Similar effects on apoptosis and cell growth were observed in PC3 cells after Hsp27 knockdown using siHsp27 (Supplementary Fig. S5). To further define the specific role of autophagy in Hsp27 inhibition-induced ER stress and apoptosis, we used siRNA to silence Atg3, a key autophagy gene essential for autophagosome formation [41]. Consistent with the CQ and 3-MA results, combined siRNA

Atg3 plus OGX-427, compared to siRNA Atg3 or OGX-427 monotherapy, increased cleaved PARP (Fig. 4D, left panel) and sub G0/G1 population (Fig. 4D, right panel). These results indicate that inhibition of stress-induced activation of autophagy increases Hsp27 knockdown-induced apoptosis and suggest that combining OGX-427 with autophagy inhibitors may enhance antitumor effects in PCa.

Combined OGX-427 plus chloroquine treatment delays PC-3 xenograft growth in vivo

PC-3 tumor-bearing mice were randomly assigned to groups treated with ScrB+PBS, ScrB +CQ, OGX-427+PBS or OGX-427+CQ when PC-3 tumors reached 100mm^3. Mean tumor volume at baseline was similar in all groups. All treatments were performed for 7 weeks. Combination therapy of OGX-427 plus CQ significantly reduced the rate of PC-3 tumor growth (Fig. 5A) compared to all other groups (P=0.0065, 0.017 and 0.038 against ScrB +PBS, ScrB+CQ and OGX-427+PBS, respectively). Combination treatment of OGX-427 plus CQ also suppressed Ki-67 expression compared to other groups (Fig. 5B), although heterogeneous immunostaining of Ki-67 suppression was apparent among individual mice (data not shown). Furthermore, OGX-427 plus CQ treated tumors had higher apoptotic rates as shown by increased TUNEL staining compared with other groups. These studies indicate that co-targeting Hsp27 and adaptive activation of autophagy significantly delays growth and increases apoptotic rates of PC-3 xenografts.

DISCUSSION

Survival proteins and signaling pathways up-regulated following anti-cancer treatment that function to inhibit cell death are of special interest in acquired treatment resistance. In particular, molecular chaperones play an important role in many stress-activated cell signaling and transcriptional regulatory networks [17, 42]. In addition, they play key roles in protein homeostasis by reducing accumulation of misfolded proteins induced by different stresses, such as heat, irradiation, oxidative stress, or anticancer therapy. Hsp27, for instance, is a stress-activated molecular chaperone commonly detected in many cancers [8–10], where it confers thermotolerance and cytoprotection by regulating steroid hormone response [43], Akt signaling [44], and NF-κB or stat3 transactivation [12–13] Hsp27 also directly inhibits components of both stress- and receptor-induced apoptotic pathways [28]. In addition, Hsp27 reduces burden of misfolded or ubiquitinated proteins by stabilizing client protein complexes [45] and enhancing proteasome activity [29]. For example, Hsp27 is associated with activated UPS and rapid degradation of UPS substrates IκBα and p27^{kip1} by the 26S proteasome [12, 46]. Stress-induced increases in Hsp27 after hormone- or chemo-therapy inhibit treatment-induced cell death, render cells more resistant to therapy, and accelerate progression [7, 12–13, 27–29].

As an important regulator of cell survival and treatment stress, Hsp27 is now recognized as therapeutic target in cancer. In this regard, selective inhibition of Hsp27 expression using siRNA [47–48] or antisense oligonucleotide [7, 15–16] -based therapy has been shown to suppress tumor growth and sensitize cancer cells to chemo- and radio-therapy. Based on these pre-clinical studies, OGX-427, a second-generation antisense inhibitor of Hsp27, has recently advanced into multicenter Phase II studies of CRPC and metastatic bladder

(ClinicalTrials.gov identifier, NCT01454089 and NCT01120470). Defining molecular mechanisms by which Hsp27 regulates cancer cell survival will provide insights into context-dependent Hsp27 action, and better guide rational combination strategies that co-target adaptive responses mediating treatment resistance.

This study set out to define the effects of Hsp27 inhibition on ER stress and proteostasis, and to evaluate biologic significance of autophagy activation under conditions of Hsp27 inhibition. We confirm that Hsp27 reduces proteasome-inhibitor induced ER stress and accumulation of misfolded/ubiquitinated protein levels, through mechanisms involving increased UPS activity and/or stabilization client-protein complexes [29, 45]. On the other hand, Hsp27 inhibition suppresses UPS activity and leads to increased levels of ubiquitinated protein with induction of ER stress and the UPR. Interestingly, Hsp27 knockdown affects the three transmembrane ER stress sensors, namely PERK (increase of p-eIF2-a, ATF-4), IRE1 (cleaved XBP1) and ATP-6 (cleaved ATF-6). These data link treatment-induced increases in Hsp27 levels to enhanced ERAD and maintenance of proteostasis. We also show, for the first time, that Hsp27 knockdown induces autophagy, and that combined inhibition of Hsp27 and autophagy further disrupts proteostasis with increased apoptosis in PCa cells. These data suggest that improved anti-cancer effects can be achieved when ER stress and unfolded protein burden overwhelms the degradation capacity of the UPS or autophagy.

While UPS and autophagy had been considered distinct and separate systems for protein clearance, recent studies suggest that they are linked especially under conditions of ER stress [23, 26, 49]. Both the UPS and autophagy are activated in response to ER stress to facilitate degradation of misfolded proteins. To reduce levels of misfolded or ubiquitinated proteins during ER stress, the UPR inhibits protein translation and promotes ERAD by stimulating the UPS. When the proteasome is inhibited, or when ER stress and unfolded protein burden overwhelms the degradation capacity of the UPS and ERAD, compensatory activation of autophagy can assist with misfolded protein clearance. This ER-activated autophagy (ERAA) is mediated by both UPR and UPR-independent mechanisms [25–26]. In this study, we show that induction of Hsp27 after proteasome inhibition functions to facilitate UPS activity and clearance of ubiquitinated proteins under conditions of ER stress; moreover, Hsp27 knockdown can suppress UPS activity and induce ER stress, apoptosis, and ERAA, illustrating a key role for Hsp27 in ER stress induced ERAD, and highlighting activation of autophagy as a compensatory cytoprotective response to maintain proteostasis.

Under many cell stress conditions, including inhibition of UPS and nutrient deprivation, autophagy is rapidly upregulated for proteostasis or alternative energy source to promote cell survival [20, 50]. However, in contrast, excessive or unquenched autophagy can lead to type II programmed cell death, which is morphologically distinct from apoptosis and usually caspase-independent [51]. Hsp27 and autophagy are activated by UPS inhibition and ER stress as adaptive responses to maintain proteostasis and block stress-induced cell death. It follows that co-targeting both Hsp27 and autophagy may increase cell death; however, it is important to recognize that the effect of manipulated autophagy can vary with intrinsic properties of the tumor and with the nature of combined therapy. Previous studies reported on combined targeting of proteasome and autophagy inhibitors in cancer [23–24]; for

example, in vitro studies in prostate cancer cells by Zhu et al [23] reported that combined inhibition of autophagy and the proteasome led to accumulation toxic intracellular protein aggregates and apoptosis. While this report demonstrates that co-targeting proteostasis pathways can enhance anti-cancer activity, it is necessary to evaluate effects of autophagy activation or inhibition in response to specific treatments and under different contexts. This study identified autophagy as an adaptive cytoprotective response to Hsp27 silencing-induced UPS inhibition, and tested whether co- targeting autophagy with Hsp27 inhibition amplified ER stress and unfolded protein burden in cancer cells to synergistically enhance treatment-induced apoptosis both in vitro and in vivo. We show that Hsp27 inhibition attenuates proteasome activity and induces the UPR similar to that seen with the classical proteasome inhibitor, MG132, and activated autophagy as a pro-survival mechanism. Co-targeted inhibition of both Hsp27 and autophagy in PCa significantly enhanced antitumor effects in vitro and in vivo.

In summary, these results suggest that Hsp27 enhances the degradative capacity of ubiquitinated proteins by the UPS following ER stress. Furthermore, Hsp27 knockdown activated autophagic flux as a cytoprotective response, and that both inhibition of Hsp27 and autophagy enhanced cell death in PCa cells in vitro and in vivo (Fig. 6). Co-targeting cytoprotective Hsp27 and autophagy represents a novel anti-cancer strategy to disrupt proteostasis and illustrates potential benefits of blocking activation of adaptive pathways to improve treatment outcomes in cancer.

Supplementary Material

Refer to Web version on PubMed Central for supplementary material.

Acknowledgments

Grant Support

This study was supported by the Terry Fox New Frontiers Program to M. E. Gleave, and the Pacific Northwest Prostate Cancer SPORE NCI CA097186 to M. E. Gleave.

References

1. Denis L, Murphy GP. Overview of phase III trials on combined androgen treatment in patients with metastatic prostate cancer. Cancer. 1993; 72:3888–3895. [PubMed: 8252511]
2. Petrylak DP, Tangen CM, Hussain MH, Lara PN Jr, Jones JA, Taplin ME, et al. Docetaxel and estramustine compared with mitoxantrone and prednisone for advanced refractory prostate cancer. N Engl J Med. 2004; 351:1513–1520. [PubMed: 15470214]
3. de Bono JS, Logothetis CJ, Molina A, Fizazi K, North S, Chu L, et al. Abiraterone and increased survival in metastatic prostate cancer. N Engl J Med. 2011; 364:1995–2005. [PubMed: 21612468]
4. Knudsen KE, Scher HI. Starving the addiction: new opportunities for durable suppression of AR signaling in prostate cancer. Clin Cancer Res. 2009; 15:4792–4798. [PubMed: 19638458]
5. Miyake H, Nelson C, Rennie PS, Gleave ME. Overexpression of insulin-like growth factor binding protein-5 helps accelerate progression to androgen-independence in the human prostate LNCaP tumor model through activation of phosphatidylinositol 3′-kinase pathway. Endocrinology. 2000; 141:2257–2265. [PubMed: 10830316]

6. Miyake H, Tolcher A, Gleave ME. Antisense Bcl-2 oligodeoxynucleotides inhibit progression to androgen-independence after castration in the Shionogi tumor model. Cancer Res. 1999; 59:4030–4034. [PubMed: 10463603]
7. Rocchi P, So A, Kojima S, Signaevsky M, Beraldi E, Fazli L, et al. Heat shock protein 27 increases after androgen ablation and plays a cytoprotective role in hormone-refractory prostate cancer. Cancer Res. 2004; 64:6595–6602. [PubMed: 15374973]
8. Arts HJ, Hollema H, Lemstra W, Willemse PH, De Vries EG, Kampinga HH, et al. Heat-shock-protein-27 (hsp27) expression in ovarian carcinoma: relation in response to chemotherapy and prognosis. Int J Cancer. 1999; 84:234–238. [PubMed: 10371339]
9. Conroy SE, Sasieni PD, Amin V, Wang DY, Smith P, Fentiman IS, et al. Antibodies to heat-shock protein 27 are associated with improved survival in patients with breast cancer. Br J Cancer. 1998; 77:1875–1879. [PubMed: 9667662]
10. Cornford PA, Dodson AR, Parsons KF, Desmond AD, Woolfenden A, Fordham M, et al. Heat shock protein expression independently predicts clinical outcome in prostate cancer. Cancer Res. 2000; 60:7099–7105. [PubMed: 11156417]
11. Parcellier A, Schmitt E, Brunet M, Hammann A, Solary E, Garrido C. Small heat shock proteins HSP27 and alphaB-crystallin: cytoprotective and oncogenic functions. Antioxid Redox Signal. 2005; 7:404–413. [PubMed: 15706087]
12. Parcellier A, Schmitt E, Gurbuxani S, Seigneurin-Berny D, Pance A, Chantome A, et al. HSP27 is a ubiquitin-binding protein involved in I-kappaBalpha proteasomal degradation. Mol Cell Biol. 2003; 23:5790–5802. [PubMed: 12897149]
13. Rocchi P, Beraldi E, Ettinger S, Fazli L, Vessella RL, Nelson C, et al. Increased Hsp27 after androgen ablation facilitates androgen-independent progression in prostate cancer via signal transducers and activators of transcription 3-mediated suppression of apoptosis. Cancer Res. 2005; 65:11083–11093. [PubMed: 16322258]
14. Vargas-Roig LM, Gago FE, Tello O, Aznar JC, Ciocca DR. Heat shock protein expression and drug resistance in breast cancer patients treated with induction chemotherapy. Int J Cancer. 1998; 79:468–475. [PubMed: 9761114]
15. Kamada M, So A, Muramaki M, Rocchi P, Beraldi E, Gleave M. Hsp27 knockdown using nucleotide-based therapies inhibit tumor growth and enhance chemotherapy in human bladder cancer cells. Mol Cancer Ther. 2007; 6:299–308. [PubMed: 17218637]
16. Matsui Y, Hadaschik BA, Fazli L, Andersen RJ, Gleave ME, So AI. Intravesical combination treatment with antisense oligonucleotides targeting heat shock protein-27 and HTI-286 as a novel strategy for high-grade bladder cancer. Mol Cancer Ther. 2009; 8:2402–2411. [PubMed: 19625496]
17. Garrido C, Brunet M, Didelot C, Zermati Y, Schmitt E, Kroemer G. Heat shock proteins 27 and 70: anti-apoptotic proteins with tumorigenic properties. Cell Cycle. 2006; 5:2592–2601. [PubMed: 17106261]
18. Kopito RR. Aggresomes, inclusion bodies and protein aggregation. Trends Cell Biol. 2000; 10:524–530. [PubMed: 11121744]
19. Rutkowski DT, Kaufman RJ. That which does not kill me makes me stronger: adapting to chronic ER stress. Trends Biochem Sci. 2007; 32:469–476. [PubMed: 17920280]
20. Harding HP, Calfon M, Urano F, Novoa I, Ron D. Transcriptional and translational control in the Mammalian unfolded protein response. Annu Rev Cell Dev Biol. 2002; 18:575–599. [PubMed: 12142265]
21. Yang Z, Klionsky DJ. Mammalian autophagy: core molecular machinery and signaling regulation. Curr Opin Cell Biol. 2010; 22:124–131. [PubMed: 20034776]
22. Codogno P, Meijer AJ. Autophagy and signaling: their role in cell survival and cell death. Cell Death Differ. 2005; 12(Suppl 2):1509–1518. [PubMed: 16247498]
23. Zhu K, Dunner K Jr, McConkey DJ. Proteasome inhibitors activate autophagy as a cytoprotective response in human prostate cancer cells. Oncogene. 2010; 29:451–462. [PubMed: 19881538]
24. Ge PF, Zhang JZ, Wang XF, Meng FK, Li WC, Luan YX, et al. Inhibition of autophagy induced by proteasome inhibition increases cell death in human SHG-44 glioma cells. Acta Pharmacol Sin. 2009; 30:1046–1052. [PubMed: 19575007]

25. Ding WX, Yin XM. Sorting, recognition and activation of the misfolded protein degradation pathways through macroautophagy and the proteasome. Autophagy. 2008; 4:141–150. [PubMed: 17986870]
26. Ding WX, Ni HM, Gao W, Yoshimori T, Stolz DB, Ron D, et al. Linking of autophagy to ubiquitin-proteasome system is important for the regulation of endoplasmic reticulum stress and cell viability. Am J Pathol. 2007; 171:513–524. [PubMed: 17620365]
27. Zoubeidi A, Zardan A, Beraldi E, Fazli L, Sowery R, Rennie P, et al. Cooperative interactions between androgen receptor (AR) and heat-shock protein 27 facilitate AR transcriptional activity. Cancer Res. 2007; 67:10455–10465. [PubMed: 17974989]
28. Zoubeidi A, Zardan A, Wiedmann RM, Locke J, Beraldi E, Fazli L, et al. Hsp27 promotes insulin-like growth factor-I survival signaling in prostate cancer via p90Rsk-dependent phosphorylation and inactivation of BAD. Cancer Res. 2010; 70:2307–2317. [PubMed: 20197463]
29. Gan N, Wu YC, Brunet M, Garrido C, Chung FL, Dai C, et al. Sulforaphane activates heat shock response and enhances proteasome activity through up-regulation of Hsp27. J Biol Chem. 2010; 285:35528–35536. [PubMed: 20833711]
30. Zoubeidi A, Ettinger S, Beraldi E, Hadaschik B, Zardan A, Klomp LW, et al. Clusterin facilitates COMMD1 and I-kappaB degradation to enhance NF-kappaB activity in prostate cancer cells. Mol Cancer Res. 2010; 8:119–130. [PubMed: 20068069]
31. Kiyama S, Morrison K, Zellweger T, Akbari M, Cox M, Yu D, et al. Castration-induced increases in insulin-like growth factor-binding protein 2 promotes proliferation of androgen-independent human prostate LNCaP tumors. Cancer Res. 2003; 63:3575–3584. [PubMed: 12839944]
32. Jiang H, Martin V, Gomez-Manzano C, Johnson DG, Alonso M, White E, et al. The RB-E2F1 pathway regulates autophagy. Cancer Res. 2010; 70:7882–7893. [PubMed: 20807803]
33. Chauhan D, Li G, Podar K, Hideshima T, Shringarpure R, Catley L, et al. The bortezomib/proteasome inhibitor PS-341 and triterpenoid CDDO-Im induce synergistic anti-multiple myeloma (MM) activity and overcome bortezomib resistance. Blood. 2004; 103:3158–3166. [PubMed: 15070698]
34. Park HS, Jun do Y, Han CR, Woo HJ, Kim YH. Proteasome inhibitor MG132-induced apoptosis via ER stress-mediated apoptotic pathway and its potentiation by protein tyrosine kinase p56lck in human Jurkat T cells. Biochem Pharmacol. 2011; 82:1110–1125. [PubMed: 21819973]
35. Yoshida H, Matsui T, Yamamoto A, Okada T, Mori K. XBP1 mRNA is induced by ATF6 and spliced by IRE1 in response to ER stress to produce a highly active transcription factor. Cell. 2001; 107:881–891. [PubMed: 11779464]
36. Scheper W, Nijholt DA, Hoozemans JJ. The unfolded protein response and proteostasis in Alzheimer disease: preferential activation of autophagy by endoplasmic reticulum stress. Autophagy. 2011; 7:910–911. [PubMed: 21494086]
37. Hartl FU, Bracher A, Hayer-Hartl M. Molecular chaperones in protein folding and proteostasis. Nature. 2011; 475:324–332. [PubMed: 21776078]
38. Mizushima N, Yoshimori T, Levine B. Methods in mammalian autophagy research. Cell. 2010; 140:313–326. [PubMed: 20144757]
39. Maiuri MC, Zalckvar E, Kimchi A, Kroemer G. Self-eating and self-killing: crosstalk between autophagy and apoptosis. Nat Rev Mol Cell Biol. 2007; 8:741–752. [PubMed: 17717517]
40. Wu Z, Chang PC, Yang JC, Chu CY, Wang LY, Chen NT, et al. Autophagy Blockade Sensitizes Prostate Cancer Cells towards Src Family Kinase Inhibitors. Genes Cancer. 2010; 1:40–49. [PubMed: 20811583]
41. Geng J, Klionsky DJ. The Atg8 and Atg12 ubiquitin-like conjugation systems in macroautophagy. 'Protein modifications: beyond the usual suspects' review series. EMBO Rep. 2008; 9:859–864. [PubMed: 18704115]
42. Whitesell L, Lindquist SL. HSP90 and the chaperoning of cancer. Nat Rev Cancer. 2005; 5:761–772. [PubMed: 16175177]
43. Carver JA, Rekas A, Thorn DC, Wilson MR. Small heat-shock proteins and clusterin: intra- and extracellular molecular chaperones with a common mechanism of action and function? IUBMB Life. 2003; 55:661–668. [PubMed: 14769002]

44. Rane MJ, Pan Y, Singh S, Powell DW, Wu R, Cummins T, et al. Heat shock protein 27 controls apoptosis by regulating Akt activation. J Biol Chem. 2003; 278:27828–27835. [PubMed: 12740362]
45. Andrieu C, Taieb D, Baylot V, Ettinger S, Soubeyran P, De-Thonel A, et al. Heat shock protein 27 confers resistance to androgen ablation and chemotherapy in prostate cancer cells through eIF4E. Oncogene. 2010; 29:1883–1896. [PubMed: 20101233]
46. Parcellier A, Brunet M, Schmitt E, Col E, Didelot C, Hammann A, et al. HSP27 favors ubiquitination and proteasomal degradation of p27Kip1 and helps S-phase re-entry in stressed cells. FASEB J. 2006; 20:1179–1181. [PubMed: 16641199]
47. Rocchi P, Jugpal P, So A, Sinneman S, Ettinger S, Fazli L, et al. Small interference RNA targeting heat-shock protein 27 inhibits the growth of prostatic cell lines and induces apoptosis via caspase-3 activation in vitro. BJU Int. 2006; 98:1082–1089. [PubMed: 16879439]
48. Kanagasabai R, Karthikeyan K, Vedam K, Qien W, Zhu Q, Ilangovan G. Hsp27 protects adenocarcinoma cells from UV-induced apoptosis by Akt and p21-dependent pathways of survival. Mol Cancer Res. 2010; 8:1399–1412. [PubMed: 20858736]
49. Pandey UB, Nie Z, Batlevi Y, McCray BA, Ritson GP, Nedelsky NB, et al. HDAC6 rescues neurodegeneration and provides an essential link between autophagy and the UPS. Nature. 2007; 447:859–863. [PubMed: 17568747]
50. Rao RV, Ellerby HM, Bredesen DE. Coupling endoplasmic reticulum stress to the cell death program. Cell Death Differ. 2004; 11:372–380. [PubMed: 14765132]
51. Gozuacik D, Kimchi A. Autophagy and cell death. Curr Top Dev Biol. 2007; 78:217–245. [PubMed: 17338918]

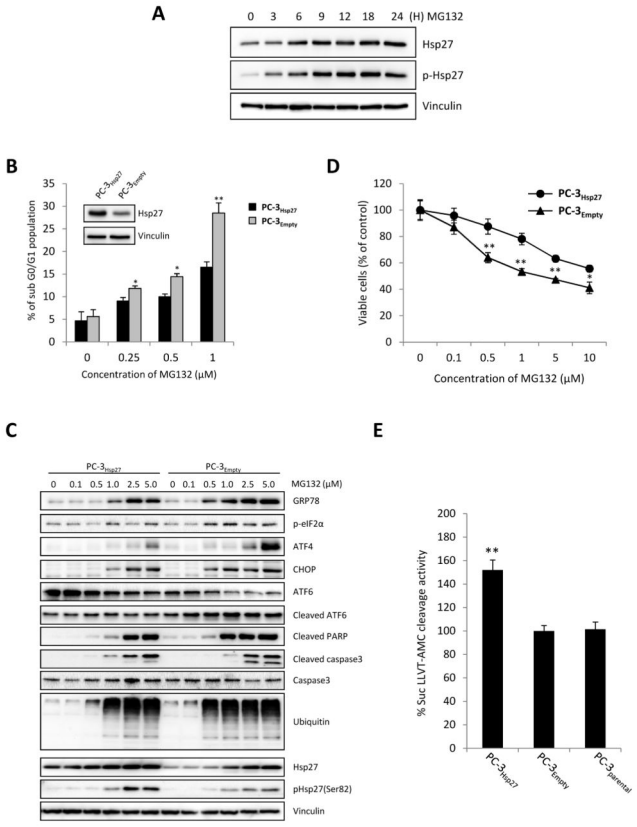

Figure 1. Hsp27 overexpression inhibits apoptosis and unfolded protein response induced by MG132 in PC-3 cells

A, PC-3 cells were treated with 5μM MG132 for the indicated time. Protein levels were analyzed by western blotting. **B** Hsp27 overexpressing stable PC-3 ($PC\text{-}3_{Hsp27}$) cells and control vector-transfected ($PC\text{-}3_{Empty}$) cells were treated with indicated concentration of MG132 for 24 hours and apoptotic rates (subG0/G1 fraction) were quantified using flow cytometry. **C,** $PC\text{-}3_{Hsp27}$ and $PC\text{-}3_{Empty}$ cells were incubated with indicated concentration of MG132. ER stress, ubiquitination and apoptosis were analyzed by changes in UPR and UPS markers expression, and caspase-3 and PARP cleavage using western blotting. **D,** $PC\text{-}3_{Hsp27}$ and $PC\text{-}3_{Empty}$ cells were treated with indicated concentration of MG132 for 24 hours and cell growth was determined by crystal violet assay. **E,** Proteasome activity was monitored in $PC\text{-}3_{Hsp27}$ and $PC\text{-}3_{Empty}$ cells and PC-3 $_{parental}$ for cleavage of the fluorescence substrate Suc-LLVY-AMC. Fluorescence was quantified using a spectrofluorometer (Fluoroskan Ascent FL, Thermo Labsystem). Bars, SD. ** differ from control ($P < 0.05$).

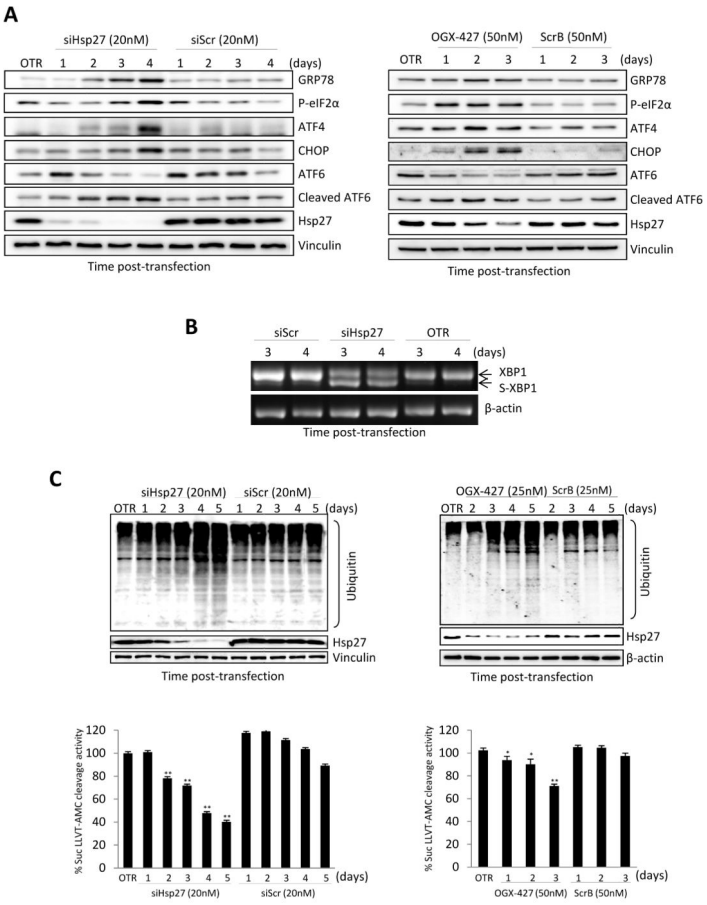

Figure 2. Hsp27 knockdown induces ER stress and decreases proteasome activity in PC-3 cells

A, PC-3 cells were transfected with either 20nM Hsp27 siRNA/Scrambled siRNA (left panel) or with 50nM OGX-427/scrambled (ScrB) control oligodeoxynucleotide (right panel). OTR indicates cells treated with oligofectamine only. Protein levels were analyzed by western blotting at different time post transfection. **B,** PC-3 cells were treated with 20nM Hsp27 siRNA or Scrambled siRNA and total RNA was extracted after 3 and 4 days post-transfection. RT-PCR analysis was performed to detect both spliced and unspliced XBP-1 mRNA. β actin was used as endogenous control. **C,** PC-3 cells were transfected with either 20 nM Hsp27 siRNA/Scr siRNA (left panel) or with 25nM OGX-427/ScrB (right panel) Ubiquitinated proteins were analyzed by western blotting using ubiquitin antibody and proteasome activity was monitored for cleavage of the Suc-LLVY-AMC substrate. Fluorescence was quantified using a spectrofluorometer (Fluoroskan Ascent FL, Thermo Labsystem). Bars, SD. ** and *, differ from control ($P < 0.01$ and $P < 0.05$, respectively).

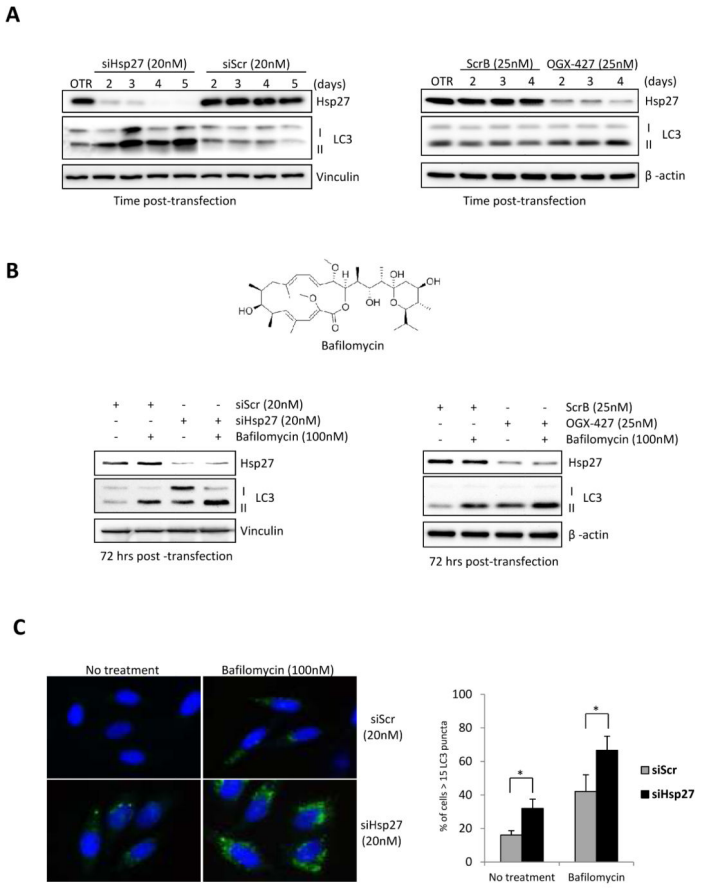

Figure 3. Hsp27 knockdown induces autophagy in PC-3 cells

A, PC-3 cells were transfected with either 20nM Hsp27 siRNA/Scr siRNA (left panel) or 25nM OGX-427/ScrB (right panel). OTR indicates cells treated with oligofectamine only. Autophagy was analyzed by western blot using LC3 antibody at different time post transfection. **B,** Chemical structure of Bafilomycin (upper panel). PC-3 cells were transfected with either 20nM Hsp27 siRNA/Scr siRNA(lower left panel) or with 25nM OGX-427/ScrB (lower right panel). Cells were exposed to 100nM Bafilomycin in the last 4 hours before protein extraction. Protein levels were analyzed by western blotting using antibodies against LC3, Hsp27 and vinculin. **C**, PC-3 cells were transfected with 20nM Hsp27 siRNA or Scrambled siRNA. Bafilomycin (100mM) was added 4 hrs before fixation. Green fluorescence puncta of endogenous were visualized by immunofluorescence (left panel) and the percentage of positive cells was quantified (right panel). Bars, SD. *, differ from control ($P < 0.01$).

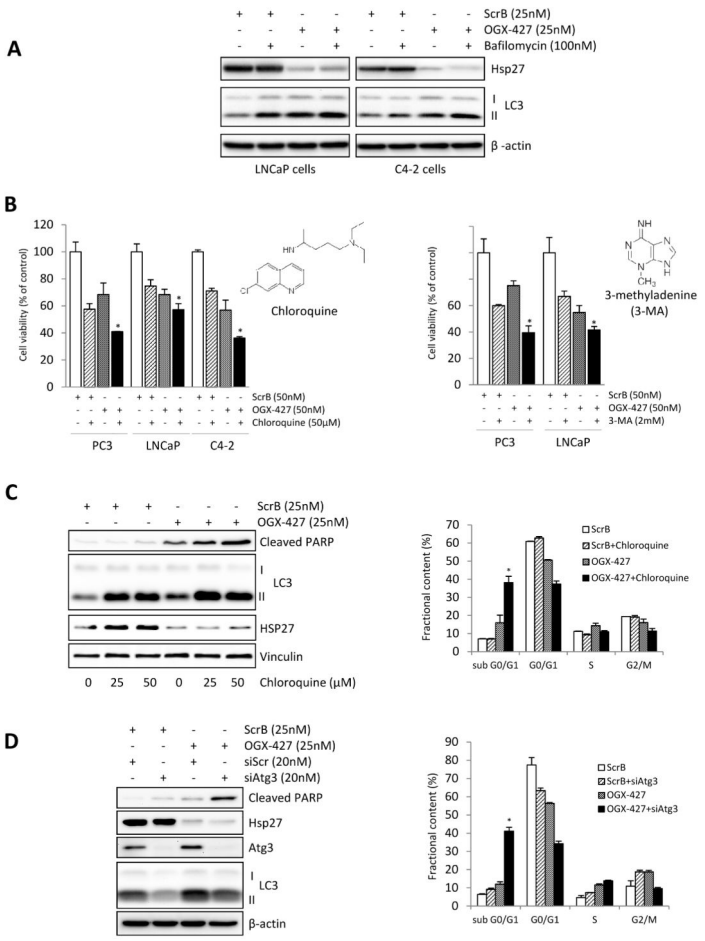

Figure 4. Inhibition of OGX-427-induced autophagy enhances prostate cancer cell apoptosis

A, LNCaP and C4-2 cells were treated with 25nM OGX-427 or ScrB, and 72 hours post-transfection were exposed for 4 hours to 100nM Bafilomycin. Autophagic flux was evaluated by western blot using LC3 antibody **B,** PCa cells were transfected with 50nM OGX-427/ScrB and treated with 50μM chloroquine (CQ) (left panel) or 2mM 3-methyladenine (3MA) (right panel) for 72 hours post transfection. Cell viability was determined by crystal violet assay. Bars, SD. *, differ from control ($P < 0.05$). CQ and 3-MA chemical structures are included in the respective panels. **C,** PC-3 cells were transfected with 25nM OGX-427 or ScrB and treated with CQ for 72 hours post transfection. Autophagic flux was evaluated by western blot using LC3 antibody and apoptosis was assessed by PARP cleavage (left panel). Percentage of sub G0/G1 population was evaluated using flow cytometry (right panel). **D**, Cells were transfected with both 25nM OGX-427 and 20nM Atg3 siRNA or the scrambled controls for 2 days. and autophagy was assessed by western blot using LC3 antibody (left panel). Cell cycle population was evaluated by flow cytometry (right panel). Bars, SD. *, differ from control ($P < 0.05$).

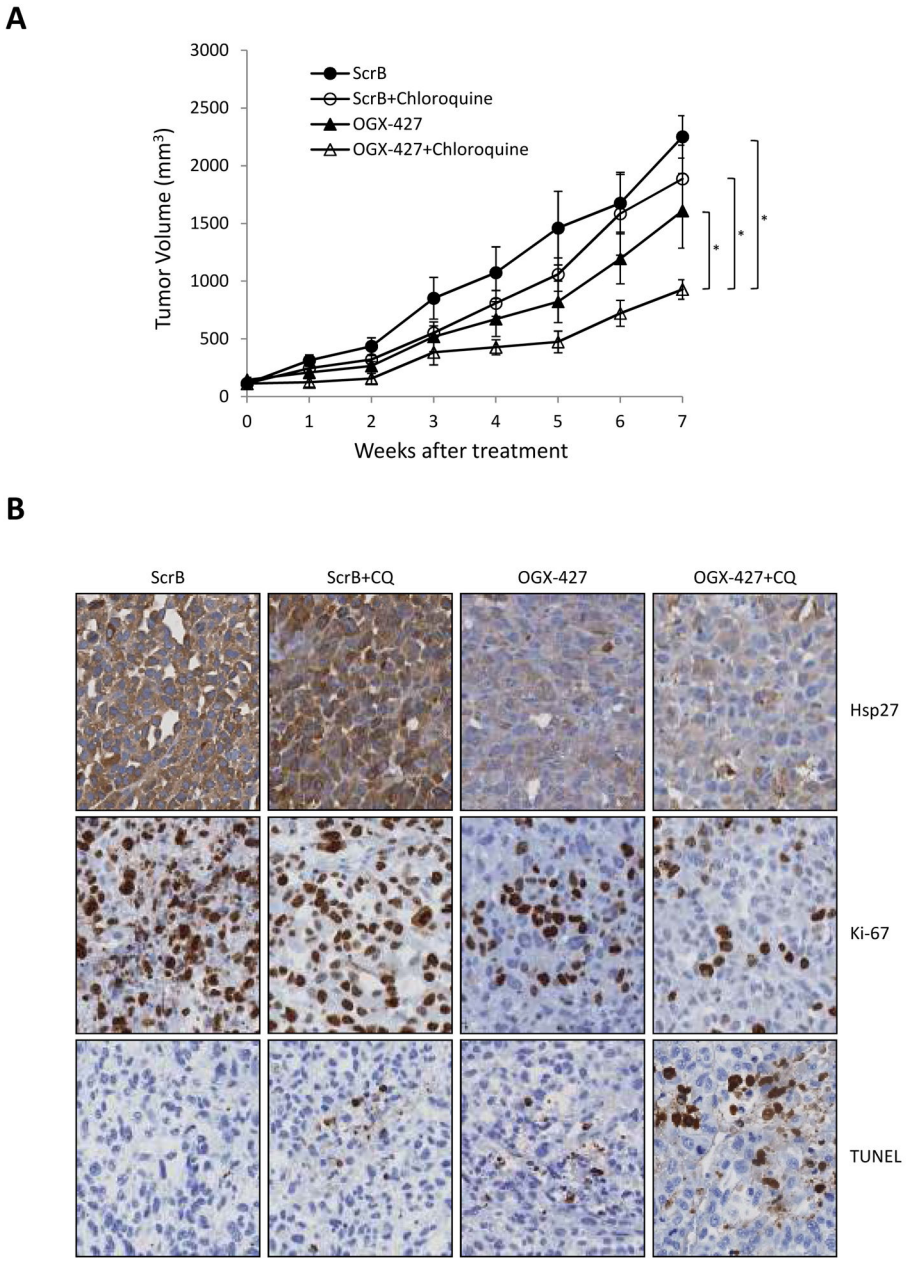

Figure 5. Combined OGX-427 plus chloroquine delays PC-3 xenograft growth in vivo

A, PC-3 cells were inoculated s.c. and when tumors reached 100mm^3, mice were treated with scrambled (ScrB) control+PBS, ScrB+chloroquine (CQ), OGX-427+PBS or OGX-427+CQ as described in Materials and Methods. Each data point represents the mean tumor volume in each group containing 8 mice ± SEM. *, differ from ScrB+PBS, ScrB+CQ or OGX-427+PBS treatment group ($P<0.05$). **B,** tumors were collected after 49 days. Hsp27, Ki-67 and TUNEL were evaluated by immunohistochemical analysis (original magnification: x200).

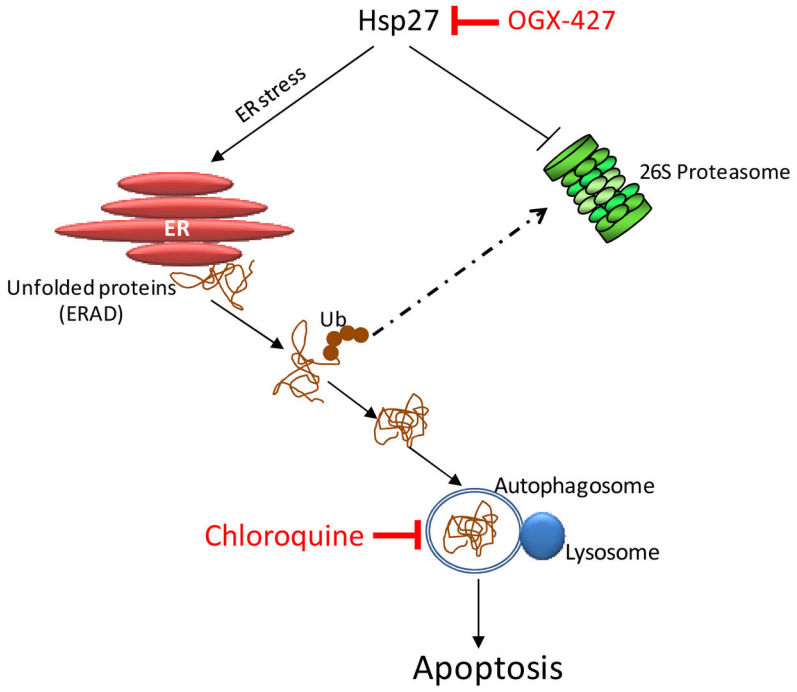

Figure 6.

Schema illustrating therapeutic strategy based on co-targeting Hsp27 and autophagy to amplify ER stress. Inhibition of Hsp27 using OGX-427 suppresses UPS activity and induces ER stress with adaptive increases in autophagy to maintain proteostasis. Co-targeting Hsp27 and autophagy disrupts proteostasis, amplifies ER stress and misfolded protein burden, thereby increasing stress-induced apoptosis.